

Cosmological models of generalized ghost pilgrim dark energy (GGPDE) in the gravitation theory of Saez-Ballester

PRIYANKA GARG¹, ARCHANA DIXIT², ANIRUDH PRADHAN³

^{1,2,3}Department of Mathematics, Institute of Applied Sciences & Humanities, GLA University, Mathura -281 406, Uttar Pradesh, India

¹E-mail: pri.19aug@gmail.com

²E-mail: archana.dixit@gla.ac.in

³E-mail: pradhan.anirudh@gmail.com

Abstract

We are studying the mechanism of the cosmic model in the presence of GGPDE and matter in LRS Bianchi type-I space-time by the utilization of new holographic DE in Saez-Ballester theory. Here we discuss all the data for three scenarios, first is supernovae type Ia union data, second is SN Ia data in combination with BAO and CMB observations and third is combination with OHD and JLA observations. From this, we get a model of our universe, where its transit state from deceleration to acceleration phase. Here we have observed that the results yielded by cosmological parameters like ρ (energy density), EoS (equation of state), squared speed of sound (v_s^2), $(\omega_D - \omega'_D)$ and $(r - s)$ plane is compatible with the recent observational data. The $(\omega_D - \omega'_D)$ trajectories in both thawing and freezing regions and the correspondence of the quintessence field with GGPDE dark energy are discussed. Some physical aspects of the GGPDE models are also highlighted.

Keywords. LRS Bianchi type-I metric; Ghost Pilgrim dark energy; time-dependent deceleration parameter; Saez-Ballester theory.

PACS Nos 98.80.Jk; 95.36.+x; 98.80.-k

1 Introduction

Nowadays it is accepted by almost every scientist in cosmology and relativity field that the cosmos is expanding till 1998, and the expansion rate is decreasing, because of gravity following up on the matter. In 1998 and following years, many groups of astronomers [1–6], in their search for the estimation of the universe expansion rate have observed some surprising results. These groups, in view of SN Ia observations, have estimated the separations and predicted the accelerated expansion of the cosmos, which is probably going to continue forever. It is anticipated by these observations that something is responsible for this acceleration. To answer this, the cosmological constant Λ , which can be the best candidate for dark energy (DE). Researchers [7, 8] have discussed locally rotationally symmetric ghost pilgrim dark energy cosmological models. In the Saez-Ballester theory of gravitation Bianchi type-II, VIII, and IX dark energy models have been discussed by [9]. Many authors [3, 10], have observed the cosmological observation that the expansion of the universe is accelerating.

To rectify the problem of DE, various DE models such as phantom, tachyon, quintessence, and Chaplyng gas have been proposed by cosmologists from time to time. The cosmology scientist usually accepts that a type of repulsive force that works as anti-gravity generated somewhere in the range of 7 billion years back is the reason for speeding up the expansion of the universe. This obscure physical entity is named as ‘dark energy’. Along with this, various researchers considered many alternative candidates as a possible source of dark energy in different scenario [11–14] in the Saez-Ballester theory. Higher-dimensional cosmic models have been discussed by [15–18].

Other than these research, a few cosmologists have studied holographic DE models as other options to DE causing late-time speeding expansion of the universe [19–30]. The hypothesis, that phantom-like DE has an adequate resistant force to cause the formation of black hole in our universe later, is the base of the proposal of pilgrim dark energy. Depending on the assumption of the generalized ghost version of the pilgrim dark energy this phenomenon has been explored. We found that the parameter (EoS) varies in both quintessence and phantom regions. Here we use linearly varying deceleration parameter

(LVDP) to test the GGPDE dark energy model in the SB scalar-tensor theory of gravity. We discuss the EoS parameter, squared speed of sound (v_s^2), $(\omega_D - \omega'_D)$ trajectories and $(r - s)$ planes to analyze the results [31]. Nowadays, due to the global property of the Universe the holographic dark energy has attracted much attention. This model depends on the holographic principle [32–39].

Furthermore, a model of dark energy named PDE (pilgrim dark energy) has been introduced by [40], and it is based on the fact that the strong repulsive force of dark energy can avoid the formation of the black hole. Instead of other types of DE, the phantom DE can play an important role. This argument coincides with the concept given by [41] which says that the mass of black holes tends to zero in the phantom energy universe approaching the Big Rip. ρ_Λ (energy density) of GGPDE is discussed and given in [42, 43]. Cosmological model in $f(R, T)$ theory of gravity are analyzed in [44, 45]. The detail expression for it is given by Eq. (13) in Sect. 3.

In the non-flat FRW universe has studied the analysis of GGPDE in [46]. The GGPDE of dark energy is also investigated in [47]. In general relativity, some Bianchi type GGPDE models have been studied by [48, 49]. Currently [50] have studied Bianchi-type- VI_0 GGPDE model. Researcher [51] have discussed the cosmological implication of interacting PDE models (with Hubble, Granda-Oliveros and generalized ghost cutoffs) Λ CDM in fractal cosmology by taking the flat universe. The GPDE model in $F(T, T_G)$ gravity with flat FRW universe have studied in [52]. Interacting GDE in a non-flat universe has been discussed by [53]

In this paper, our aim is to investigate the LRS Bianchi type-I GGPDE model in the Saez-Ballester theory of gravitation. The paper has the following structure. Sect. 2, presents deviation of field equations in Saez-Ballester's theory. In Sect. 3, we obtained the metric and field equations for Bianchi type-I space times. In Sect. 2, we describe calculations of some other physical and kinematic parameters. Interpretation of the results obtained is written in Sect. 3. In Sect. 4, we deal the the stability analysis of the solution. State-finder p (r, s) have been obtained in Sect. 5. Sound speed is discussed in Sect. 6. The analysis of $\omega_D - \omega'_D$ in Sect. 7. Correspondence of quintessence field in Sect. 8. In the last part Sect. 9, conclusion and the description are given.

2 Explicit field equations in Saez-Ballester theory

The field equations founded by Saez-Ballester [1] for the combined scalar and tensor fields are:

$$R_{ij} - \frac{1}{2}Rg_{ij} - w\phi^n(\phi_{,i}\phi_{,j} - \frac{1}{2}g_{ij}\phi_{,k}\phi^{,k}) = -(T_{ij} + \bar{T}_{ij}), \quad (1)$$

and the equations which are satisfied by ϕ (scalar field) :

$$2\phi^n\phi_{;i}^i + n\phi^{n-1}\phi_{,k}\phi^{,k} = 0. \quad (2)$$

In addition the conservation equation is

$$(T_{ij} + \bar{T}_{ij})_{;j} = 0. \quad (3)$$

Here, R is the Ricci scalar, R_{ij} is the Ricci tensor, n and w are arbitrary dimensionless constants and $8\pi G = C = 1$ in the relativistic units.

Now, we define T_{ij} and \bar{T}_{ij} which are energy-momentum tensors for matter and holographic dark energy such as

$$T_{ij} = \rho_m u_i u_j. \quad (4)$$

$$\bar{T}_{ij} = (\rho_\Lambda + p_\Lambda)u_i u_j - p_\Lambda g_{ij}. \quad (5)$$

Here ρ_Λ is the holographic dark energy, ρ_m is the energy densities of matter and p_Λ is the pressure of holographic dark energy.

Now LRS Bianchi type-I metric takes the form

$$ds^2 = dt^2 - a_1^2 dx^2 - a_2^2 (dy^2 + dz^2), \quad (6)$$

where $a_1(t)$ and $a_2(t)$ are time dependent functions.

Now using Eqs. (1), (2), (4), (5) and co moving coordinates for the metric (6) form the following equations

$$\frac{2\ddot{a}_2}{a_2} + \frac{\dot{a}_2^2}{a_2^2} - \frac{w}{2}\phi^n\dot{\phi}^2 = -p_\Lambda, \quad (7)$$

$$\frac{\ddot{a}_1}{a_1} + \frac{\ddot{a}_2}{a_2} + \frac{\dot{a}_1\dot{a}_2}{a_1a_2} - \frac{w}{2}\phi^n\dot{\phi}^2 = -p_\Lambda, \quad (8)$$

$$\frac{2\dot{a}_1\dot{a}_2}{a_1a_2} + \frac{\dot{a}_2^2}{a_2^2} + \frac{w}{2}\phi^n\dot{\phi}^2 = \rho_m + \rho_\Lambda, \quad (9)$$

$$\ddot{\phi} + \dot{\phi} \left(\frac{\dot{a}_1}{a_1} + 2\frac{\dot{a}_2}{a_2} \right) + \frac{n}{2} \frac{\dot{\phi}^2}{\phi} = 0. \quad (10)$$

Here overhead dot indicates differentiation with respect to t . Here the EoS parameter of dark energy is $p_\Lambda = \omega_\Lambda\rho_\Lambda$.

The conservation equation of the matter and dark energy is

$$\rho_m + \rho_\Lambda + \left(\frac{\dot{a}_1}{a_1} + 2\frac{\dot{a}_2}{a_2} \right) (\rho_m + \rho_\Lambda + p_\Lambda) = 0. \quad (11)$$

3 Solutions of the field equations

Now, we solve the field equations Eqs. (7)- (10), which are a system of four independent field equations in six unknowns parameters $a_1, a_2, \rho_\Lambda, \rho_m, p_\Lambda$ and ϕ . Therefore, to obtain explicit solutions of the system, For solving the above highly non-linear differential equations we have required the following physically significant conditions, which are relating to these parameters.

We assume that the expansion scaler (θ) is proportional to shear scalar (σ). The condition leads to $\frac{\dot{a}_1}{a_1} = m\frac{\dot{a}_2}{a_2}$, which yields [54]

$$a_1 = a_2^m. \quad (12)$$

The motivation behind assuming this condition is given [55].

The energy density of GGPDE (ρ_Λ) defined by [42]

$$\rho_\Lambda = M_{pl}^2(\alpha_1 H + \alpha_2 H^2)^\kappa, \quad (13)$$

where H is the Hubble parameter, $M_{pl}^2 = \frac{1}{8\pi G}$ is the reduced Plank mass, κ is PDE parameter, and α_1, α_2 are two arbitrary dimensionless parameters.

Motivated by the recent observational data, we consider the deceleration parameter q as a linear function of Hubble parameter H as [56]

$$q = -\frac{a\ddot{a}}{\dot{a}^2} = \alpha + \beta H. \quad (14)$$

Here α and β are arbitrary constants.

Solving Eq. (14), $\alpha = -1$, the various authors [56–59] obtained the solution as:

$$a = \exp\left(\frac{1}{\beta}\sqrt{2\beta t + k}\right), \quad (15)$$

where k is an integrating constant. Recently this Eq. (15) is used by many authors [56–59].

We have found the value of deceleration parameter from Eq. (19)

$$q = -1 + \frac{\beta}{\sqrt{2\beta t + k}}. \quad (16)$$

As it has been observed that the expansion rate of the universe is time dependent instead of being constant. So we will use $\alpha = -1$, for which we find the time dependent value of DP and not $\alpha \neq -1$ as it results into constant DP $q = -1$.

The average scale factor for the metric (6) is define as $a = (a_1 a_2^2)^{\frac{1}{3}}$.

Using the above relation and Eqs. (12) and (15), we get

$$a_1 = \exp \left[\frac{3m}{(m+2)} \frac{1}{\beta} \sqrt{2\beta t + k} \right]. \quad (17)$$

Using above in Eq. (12), we get

$$a_2 = \exp \left[\frac{3}{(m+2)} \frac{1}{\beta} \sqrt{2\beta t + k} \right]. \quad (18)$$

Therefore, the geometry of the metric (6) comes out to be

$$ds^2 = dt^2 - \left(\exp \left[\frac{6m}{(m+2)} \frac{1}{\beta} \sqrt{2\beta t + k} \right] \right) dx^2 - \left(\exp \left[\frac{6}{(m+2)} \frac{1}{\beta} \sqrt{2\beta t + k} \right] \right) (dy^2 + dz^2). \quad (19)$$

Now from equations (10), (17) and (18) the scalar field is obtained as:

$$\phi^{\frac{(n+2)}{2}} = \frac{(n+2)}{2} \left[\exp \left(\frac{-3}{\beta} \sqrt{2\beta t + k} \right) \left(\frac{-c_1}{3} \sqrt{2\beta t + k} - \frac{\beta}{9} \right) + c_2 \right], \quad (20)$$

where c_1 and c_2 are constants of integration.

Now we find the energy density of GGPDE from (13) as

$$\rho_\Lambda = \left[\frac{1}{(\sqrt{2\beta t + k})} \left(\alpha_1 + \alpha_2 \frac{1}{\sqrt{2\beta t + k}} \right) \right]^\kappa. \quad (21)$$

From Eqs. (9), (17), (18), (20) and (21) we find the energy density of the matter as

$$\rho_m = \frac{9(2m+1)}{(m+2)^2(2\beta t + k)} + \frac{\omega c_1^2}{2} \exp \left[\frac{-6}{\beta} \sqrt{2\beta t + k} \right] - \left[\frac{1}{(\sqrt{2\beta t + k})} \left(\alpha_1 + \alpha_2 \frac{1}{\sqrt{2\beta t + k}} \right) \right]^\kappa. \quad (22)$$

The expression for pressure of holographic dark energy is obtained as:

$$p_\Lambda = \left(\frac{-3\beta(m+1)}{(m+2)(2\beta t + k)^{\frac{3}{2}}} + \frac{9(m^2 + m + 1)}{(m+2)^2(2\beta t + k)} - \frac{\omega c_1^2}{2} \exp \left[\frac{-6}{\beta} \sqrt{2\beta t + k} \right] \right). \quad (23)$$

From Eqs. (23) and (21), we obtain equation of state parameter of dark energy ω_Λ

$$\omega_\Lambda = \frac{\left(\frac{-3\beta(m+1)}{(m+2)(2\beta t + k)^{\frac{3}{2}}} + \frac{9(m^2 + m + 1)}{(m+2)^2(2\beta t + k)} - \frac{\omega c_1^2}{2} \exp \left[\frac{-6}{\beta} \sqrt{2\beta t + k} \right] \right)}{\left[\frac{1}{(\sqrt{2\beta t + k})} \left(\alpha_1 + \alpha_2 \frac{1}{\sqrt{2\beta t + k}} \right) \right]^\kappa}. \quad (24)$$

The density parameter Ω is given by

$$\Omega = \frac{\rho_\Lambda + \rho_m}{3H^2}, \quad (25)$$

which is equal to

$$\Omega = \left(\frac{3(2m+1)}{(m+2)^2} + \frac{\omega c_1^2}{6} (2\beta t + k) \exp \left[\frac{-6}{\beta} \sqrt{2\beta t + k} \right] \right). \quad (26)$$

4 Experimental data and calculations of parameters

From Eq. (14), we have $q_0 = -1 + \beta H_0$, where q_0 and H_0 are the present values of DP and Hubble parameter respectively.

Also, we have $H = \frac{\dot{a}}{a} = \frac{1}{\sqrt{2\beta t + k}}$, so that $H_0 = \frac{1}{\sqrt{2\beta t_0 + k}}$. Using $H_0.t_0 = 1$, we can get $H_0 = \frac{1}{\sqrt{2\frac{\beta}{H_0} + k}}$. Solving it for k , we have $k = \frac{1}{H_0} \left[\frac{1}{H_0} - 2\beta \right]$.

Here three cases has been considered which is based on three different data:

Case I: Based on supernovae type la union data

Now, taking $q_0 = -0.73$ and $H_0 = 73.8$ [60], we obtain $\beta = 0.003658$. For these values β and H_0 , we get $k = 0.000084$.

Case II: Based on SN la data in combination with BAO and CMB observations

Taking $q_0 = -0.54$ and $H_0 = 73.8$ [61] , we obtain $\beta = 0.0062$. For these values β and H_0 , we get $k = 0.00001$.

Case III: Based on current data in combination with OHD and JLA observations

Taking $q_0 = -0.52$ and $H_0 = 69.2$ [62], we obtain $\beta = 0.0069$. For these values β and H_0 , we get $k = 0.0000083$.

q_0	H_0	β	k	Reference
-0.73	73.8	0.003658	0.000084	[60]
-0.54	73.8	0.0062	0.00001	[61]
-0.52	69.2	0.0069	0.0000083	[62]

Table 1: For different observed values of deceleration parameter (q_0), Hubble parameter (H_0), values of (β, k).

In this paper we have drawn all the figures for these different values of (β, k) as (0.003658, 0.000084), (0.0062, 0.00001), and (0.0069, 0000083) respectively.

The Hubble parameter H , scalar expansion θ , shear scalar σ and the average anisotropy parameter A_m are calculated for our model which is defined as:

$$H = \frac{\dot{a}}{a} = \frac{1}{\sqrt{2\beta t + k}} \tag{27}$$

$$\theta = 3H = \frac{3}{\sqrt{2\beta t + k}} \tag{28}$$

$$\sigma^2 = \frac{1}{2} \left[(H_1^2 + 2H_2^2) - \frac{\theta^2}{3} \right] = \frac{3(m-1)^2}{(m+2)^2(2\beta t + k)} \tag{29}$$

$$A_m = \frac{1}{3} \sum_{i=1}^3 \left(\frac{\Delta H_i}{H} \right)^2 = \frac{2(m-1)^2}{(m+2)^2} \tag{30}$$

5 Results and discussions

Figure 1(a) depicts cosmological model with DP (q) versus time t . It can be observe that for $k = 0.000084$ and $\beta = 0.0036$, our models are only in accelerating phase, but for $k = 0.000012$ and $\beta = 0.0064$, the model shows a transition phase from +ve to -ve deceleration parameter q i. e. our model is transforming from $q > 0$ (deceleration) to $q < 0$ (acceleration) phases. Similarly for the current data $k = 0.0000083$ and $\beta = 0.0069$ models is decelerating to the accelerating phase transforming. Since DP (q) value lies between the range $-1 < q < 0$ and the expansion of the current universe in accelerating are exposed by SNe 1a data. So the value of the decelerating parameter is consistent with recent observations.

The value of scale factor ($a(t)$) in the form of z is $a(t) = \frac{a_0}{1+z}$, where a_0 is the current value of scale factor. From Eq. (19), we find $\ln(a) = \frac{\sqrt{2\beta t + c_1}}{\beta}$. And we also obtain the value of $\ln(a)$ in term of redshift z , i.e. $\ln(a) = \ln(a_0) - \ln(1+z)$ from $a(t) = \frac{a_0}{1+z}$. Using this value in Eq. (20), we obtain $q(z) = -1 + \frac{1}{\ln(a_0) - \ln(1+z)}$.

For our derived model variation of redshift z versus t (cosmic time) is demonstrate by figure 1(b). In this figure we have seen that for this value a_0 redshift z is a monotonic decreasing with increase of t . So it can be say that for our model derived z starts with a small positive value at t equal to 0 and z tends to -1 as t tends to ∞ .

Figure 1(c) shows $q - z$ plane for generalized q -parametrization given by $q(z) = -1 + \frac{1}{\ln(\frac{a_0}{1+z})}$ for three cases of (β, k) i.e. ($\beta = 0.003658, k = 0.000084, \beta = 0.0062, k = 0.00001$ and $\beta = 0.0069, k = 0.0000083$) and we get the value of a_0 . For plot the graph we use these values.

In the figure we have discovered that $q(z)$ expansion undergoes a smooth transition from a decelerated stage to accelerated stage and $q \rightarrow -1$ as $z \rightarrow -1$. Currently, [63, 64] have discovered the change redshift from decelerating to accelerating in modified gravity cosmology. SNe type Ia dataset has given the progress from past deceleration to ongoing acceleration. More recently, in 2004 the HZSNS team have found $z_t = 0.46 \pm 0.13$ at (1σ) c.l. [4]. It is improved in 2007 to $z_t = 0.43 \pm 0.07$ at (1σ) c.l. [5]. SNLS [65] compiled by [66], provide a progress redshift $z_t \sim 0.6(1\sigma)$ in improved agreement with the flat Λ CDM model ($z_t = (2\Omega_\Lambda/\Omega_m)^{\frac{1}{3}} - 1 \sim 0.66$).

Moreover the reconstruction of $q(z)$ is done by the joined ($SNIa + CC + H_0$), which have obtained the transition redshift $z_t = 0.69^{+0.09}_{-0.06}, 0.65^{+0.10}_{-0.07}$ and $0.61^{+0.12}_{-0.08}$ within (1σ) [67]. which are seen as well consistent with past outcomes [68–72] including the Λ CDM expectation $z_t \approx 0.7$. Another limit of transition redshift is $0.6 \leq z_t \leq 1.18$ (2σ , joint examination) [73].

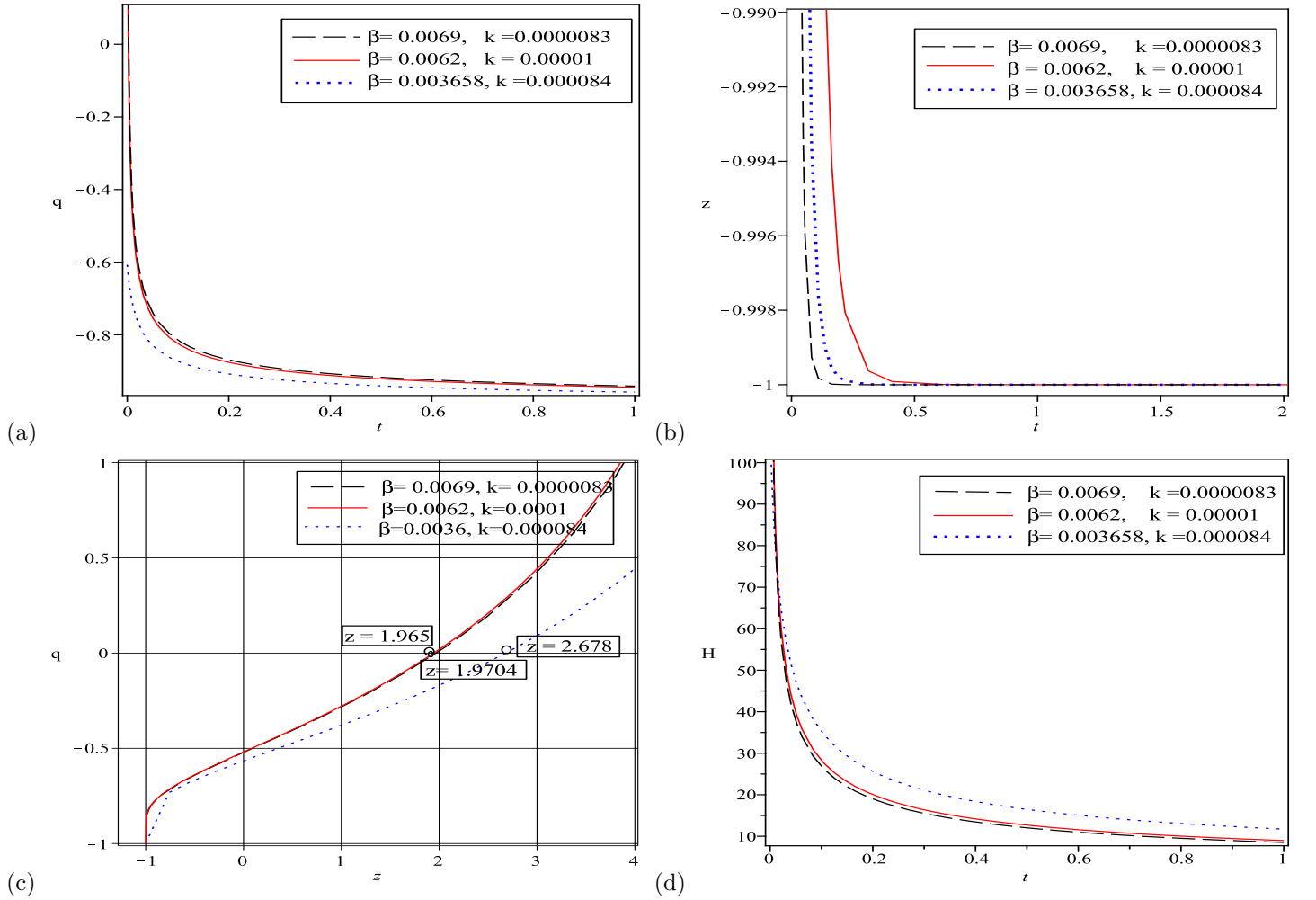


Figure 1: (a)The graph between q versus t , (b) The graph between z versus t , (c)The graph between q versus red shift z , (d) The graph of Hubble parameter H versus cosmic time t .

From the figure it is clear that the transition redshift from decelerated to accelerated expansion occurs at $z_t \cong 1.965$, $z_t \cong 1.9704$ and $z_t \cong 2.678$ (see Fig. 1c) for above three cases which are found to be well consistent with the Type Ia supernovae Hubble diagram, including the farthest known supernova SNI99ff at $z \approx 1.7$ [74, 75]).

Figure 1(d) depicts between the Hubble parameter and time. We observed that $H \rightarrow 0$ as $t \rightarrow \infty$ as per theoretical desire.

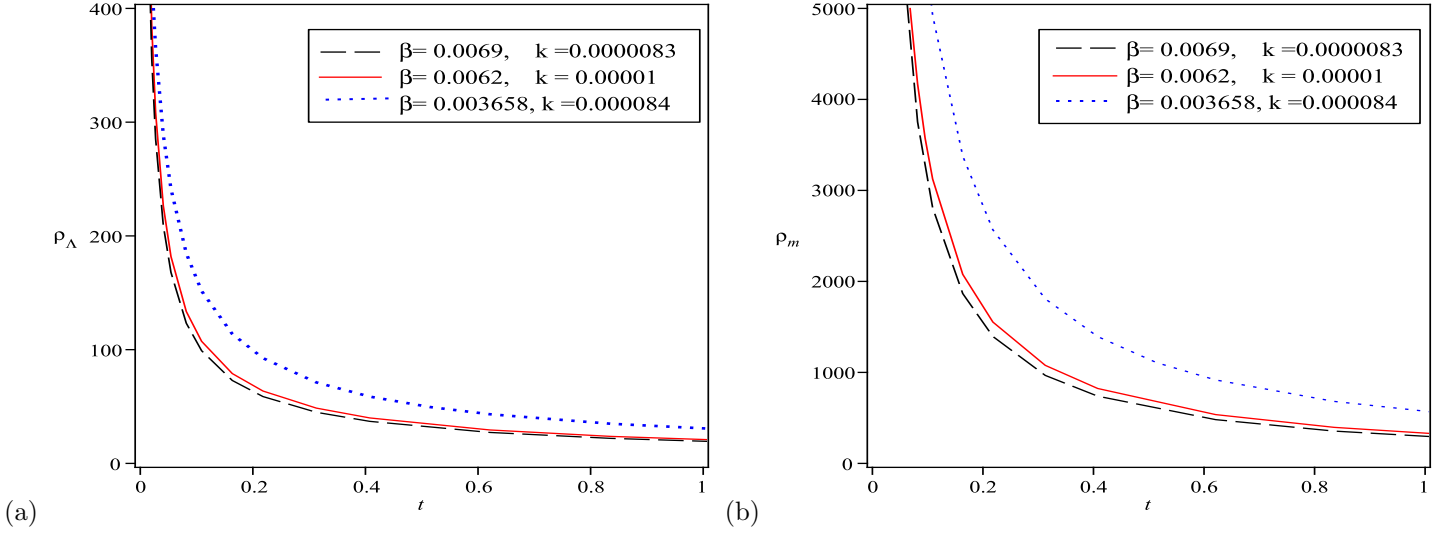


Figure 2: (a) The plot of energy density of GGPDE versus time t , (b) The plot of energy density of matter versus cosmic time t .

We observe that from Eq. (25) and its corresponding figure 2(a), shows that for all three cases ρ_Λ remains positive during the cosmic evolution. Similarly from Eq. (26) and its corresponding figure 2(b), it indicates that the energy density of matter ρ_m decreases with increase of time and it also remains positive for all values of k and β during the cosmic evolution. We can see first it decreased sharply and then gradually and approach to a small positive values at the present epoch. ρ_Λ and ρ_m tends to 0 as $t \rightarrow \infty$. Since decrease in density implies the increase in volume i.e. our derived model represents the expansion of the universe.

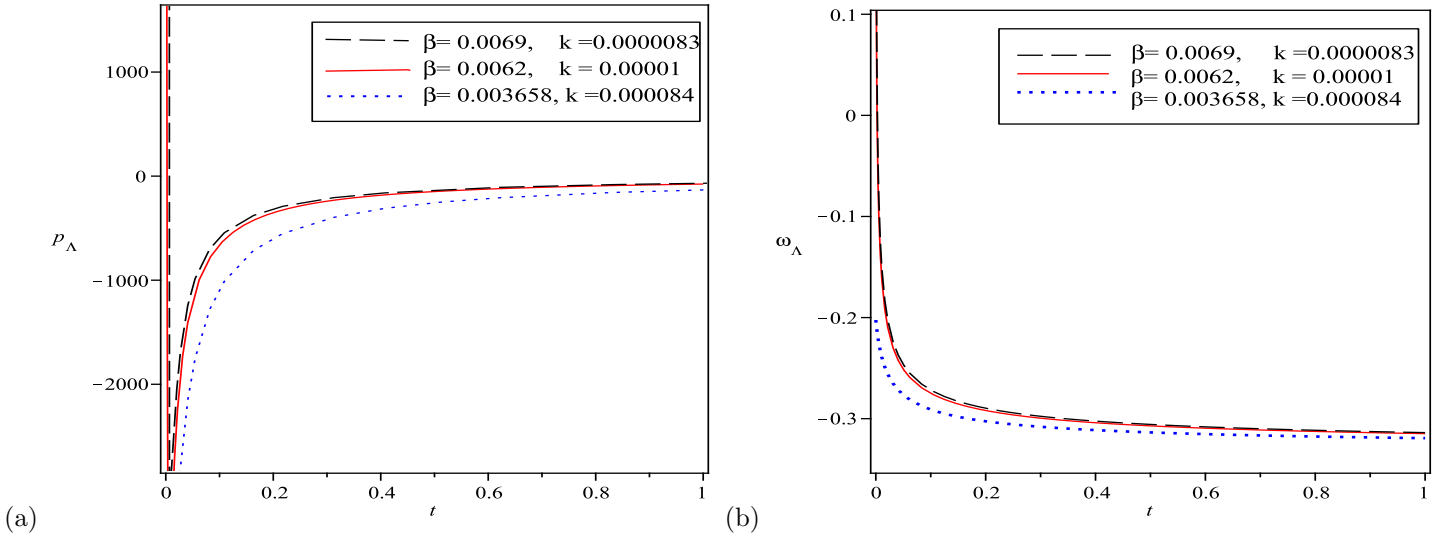


Figure 3: (a) The plot of pressure p_Λ of GGPDE versus time t , (b) The plot of equation of state parameter ω_Λ versus cosmic time t

Figure 3(a) depicts pressure p_Λ versus time t . It is observed that the value of isotropic pressure was positive in the beginning. Later it decreased rapidly and then it remained negative throughout evolution. This negative pressure put the equation of state $\omega = \frac{p_\Lambda}{\rho_\Lambda} < 0$, as prescribed by recent observations and it may be a cause of the accelerated expansion of the universe. Figure 3(b) demonstrate the equation of state parameter ω for all three observational value.

From Eq. (28) and its corresponding figure 3(b), it is clearly shown that for all three data firstly EoS parameter ω_Λ was positive then decreased sharply and approach to a small negative value at the present epoch. The EoS parameter of DE may begin in phantom $\omega \leq -1$ or quintessence $\omega \geq -1$ region and tends to -1 by exhibiting various patterns as t increases. Here ω_Λ is less than -1 so there is aphantom region. i.e. ω_Λ evolves with negative and its range is in nice agreement with large

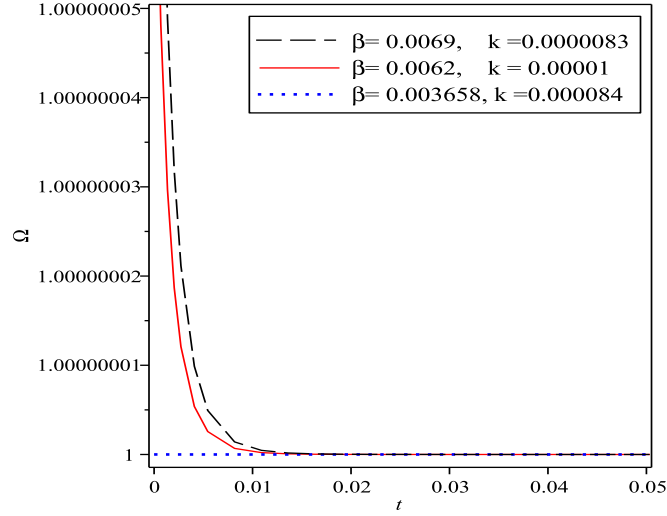


Figure 4: Total energy density (Ω) of GGPDE versus time t .

scale structure data [76].

Figure 4 shows the graph of Ω versus t for all three values of (β, k) . We observe that (Ω) approaches close to 1 as $t \rightarrow \infty$ i.e. the total energy density of GGPDE models at present is 1.

Jerk is the rate of change of acceleration; that is, the time derivative of acceleration. Many authors [77, 78] have indicated the significance of jerk as a tool to reconstruct the cosmological models. Recently, [79, 80] have discussed the parametrization of time evolving jerk parameter models.

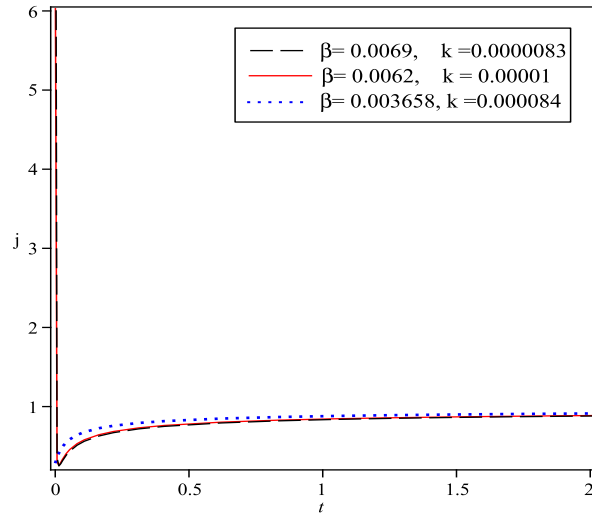


Figure 5: Jerk parameter of GGPDE versus time t .

We hereby define the cosmic Jerk parameter such as:

$$j = -\frac{1}{aH^3} \left(\frac{d^3 a}{dt^3} \right) = q + q^2 - \frac{\dot{q}}{H} \quad (31)$$

$$j = \frac{3\beta^2}{2\beta t + k} - \frac{3\beta}{\sqrt{2\beta t + k}} + 1 \quad (32)$$

Figure 5 demonstrate that firstly the graphs decrease rapidly for all three value $\beta = 0.0069$ & $k = 0.0000083$; $\beta = 0.0062$ & $k = 0.00001$, and $\beta = 0.0069$ & $k = 0.0000083$ then approach to 1 through the evolution history i.e. the best suitable value of j is very close to 1 is showed by this figure and it clearly indicates that the model is extremely close to Λ CDM model. A well known constrained value of jerk parameter is found by statistical analysis with different observational data sets like BAO (baryon acoustic oscillation data), SNe (Ia supernova data) and OHD (observational Hubble parameter data). A well known constrained value of jerk parameter is found by statistical analysis with different observational data sets like BAO (baryon acoustic oscillation data), SNe (Ia supernova data) and OHD (observational Hubble parameter data) and the model remains at very close proximity of the Λ CDM.

6 Squared sound speed

Many authors [81,82] have examined the speed of sound constraints of dynamic DE models with EoS parameter varying in time and concluded that the speed of the sound constraint of DE is very low. If the speed of sound lies between zero and 1, the system is stable.

Now for any fluid, the adiabatic square sound speed is described as $v_s^2 = dp/d\rho$. Besides the positivity of v_s^2 , the condition of causality must satisfied. Causality means the speed of sound should not surpass the speed of light. Since we use relativistic units where $c = G = 1$, the speed of sound should be within the range $0 \leq dp/d\rho \leq 1$.

$$v_s^2 = \frac{\left(\frac{-9\beta^2}{(2m+1)(2\beta t+k)^{\frac{3}{2}}} + \frac{18\beta}{(2m+1)^2(2\beta t+k)^{\frac{3}{2}}} - \frac{\omega c_1^2(1+\frac{2}{m})}{\sqrt{2\beta t+k}} \exp\left[\frac{-2(m+2)}{m} \frac{1}{\beta} \sqrt{2\beta t+k}\right] \right)}{\left[\kappa \left(\frac{1}{\sqrt{2\beta t+k}} \left(\alpha_1 + \alpha_2 \frac{1}{\sqrt{2\beta t+k}} \right) \right)^\kappa \left[\frac{1}{\sqrt{2\beta t+k}} \left(\alpha_1 + \alpha_2 \frac{1}{\sqrt{2\beta t+k}} \right) \right] \times \left(\frac{-\beta}{(2\beta t+k)} \left(\alpha_1 + \alpha_2 \frac{1}{\sqrt{2\beta t+k}} \right) - \frac{\alpha_2\beta}{(2\beta t+k)} \right) \right]}. \quad (33)$$

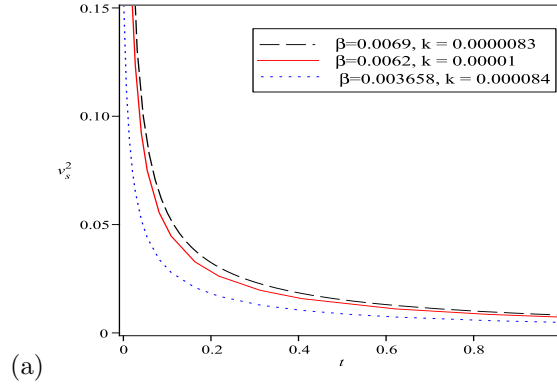


Figure 6: The graph between v_s^2 versus time t is shown

Figure (6) depict the plots of speed of sound with time for all three values of β and k . We observe that $v_s < 1$ throughout the evolution of the universe. From the figure, it is sorted out that throughout the universe evolution sound speed remains less than light velocity ($c = 1$).

7 The $\omega_D - \omega'_D$ analysis

Caldwell and Linder [83] implemented a plane analysis of $\omega_D - \omega'_D$. This analysis is a utile shaft for separating vDE models by trajectories on their planes. The method is also applied to the quintessence model that leads to two forms of its plane, i.e. the area belongs to the $(\omega_D < 0, \omega'_D > 0)$ region refers to the thawing region while the area below the $(\omega_D < 0, \omega'_D < 0)$ region indicates the freezing region. Later this analysis was extended by many researchers to other dynamic DE models [84–87]. Clearly, a fixed point at $(-1, 0)$ is the Λ CDM model in the ω_D phase space. To discuss GGPDE model, here we use this analysis.

On differentiating Eq. (24) w.r.t. $\ln a$ and find the value of ω'_D as

$$\begin{aligned}
\omega'_D = & \left[\frac{\left(\frac{-9\beta^2}{(2m+1)(2\beta t+k)^{\frac{3}{2}}} + \frac{18\beta}{(2m+1)^2(2\beta t+k)^{\frac{3}{2}}} - \frac{\omega c_1^2(1+\frac{2}{m})}{\sqrt{2\beta t+k}} \exp\left[\frac{-2(m+2)}{m} \frac{1}{\beta} \sqrt{2\beta t+k}\right] \right)}{\left[\frac{1}{(\sqrt{2\beta t+k})} \left(\alpha_1 + \alpha_2 \frac{1}{\sqrt{2\beta t+k}} \right) \right]^\kappa} \right. \\
& \left. \frac{\left(\frac{3\beta^2}{(2m+1)(2\beta t+k)^{\frac{3}{2}}} - \frac{9}{(2m+1)^2(2\beta t+k)} + \frac{\omega c_1^2}{2} \exp\left[\frac{-2(m+2)}{m} \frac{1}{\beta} \sqrt{2\beta t+k}\right] \right)}{\left[\frac{1}{(2\beta t+k)^{\frac{3}{2}}} \left(\alpha_1 + \alpha_2 \frac{1}{\sqrt{2\beta t+k}} \right) \right]^{\kappa+1}} \right] \times \\
& \left(\frac{-\beta}{\sqrt{2\beta t+k}} \left(\alpha_1 + \alpha_2 \frac{1}{\sqrt{2\beta t+k}} \right) - \frac{\alpha_2 \beta}{\sqrt{2\beta t+k}} \right). \tag{34}
\end{aligned}$$

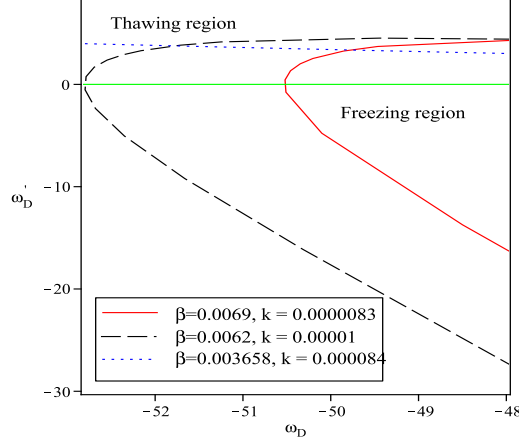


Figure 7: The plot of evolutionary trajectories of the $\omega_D - \omega'_D$

We constructed the $\omega_D - \omega'_D$ plane by plotting ω'_D versus ω_D as shown in Fig. 7. It can be observed that the curves lead to both freezing and thawing regions for three values of parameter β and k . Nevertheless, the trajectories differ for the supernova Ia union data in the thawing region and for the BAO & CMB observations and OHD & JLA observation curves correspond to both the freezing and thawing areas. Nevertheless, our model's trajectories differ mostly in the freezing zone, as indicated by observational data (the expansion of the universe is comparatively more accelerated in the freezing area).

8 Correspondence of quintessence field in GGPDE

In the presence of non-relativistic matter represented by a barotropic perfect fluid, let us consider quintessence. The quintessence field action is given in [88]

$$S = \int \sqrt{-g} d^4x \left[\frac{1}{2} M_{pl}^2 R - \frac{1}{2} g^{ij} \phi_{;i} \phi_{;j} - V(\phi) \right] + S_m, \tag{35}$$

where M_{pl} is the reduced Planck mass, g^{ij} is the metric whereas g is the metric determinant and R is the scalar Ricci. In the above, S_m is the action standard field, $V(\phi)$ is the potential for the quintessence field ϕ and $\phi_{;i}$ is the covariant derivative of ϕ .

By varying the action given in Eq. (35) with respect to the metric and ϕ respectively we obtain,

$$3M_{pl}^2 H^2 = \rho_m + \frac{\dot{\phi}^2}{2} + V(\phi), \tag{36}$$

$$M_{pl}^2 (2\dot{H} + 3H^2) = -\frac{\dot{\phi}^2}{2} + V(\phi). \tag{37}$$

On solving Eqs. (36) and (37), we obtain potential versus cosmic time t .

$$V(\phi) = \frac{M_{pl}^2}{2} \left(\frac{-2\beta}{(2\beta t + k)^{\frac{3}{2}}} + \frac{6}{(2\beta t + k)} \right) - \frac{1}{2} \left[\frac{\alpha_1}{(\sqrt{2\beta t + k})} + \frac{\alpha_2}{2\beta t + k} \right]^\kappa, \quad (38)$$

and scalar field versus time t is

$$\dot{\phi}^2 = \frac{6M_{pl}^2}{(2\beta t + k)} - \frac{3}{2} \left[\frac{1}{(\sqrt{2\beta t + k})} \left(\alpha_1 + \alpha_2 \frac{1}{\sqrt{2\beta t + k}} \right) \right]^\kappa + \frac{M_{pl}^2}{2} \left(\frac{2\beta}{(2\beta t + k)^{\frac{3}{2}}} - \frac{6}{(2\beta t + k)} \right), \quad (39)$$

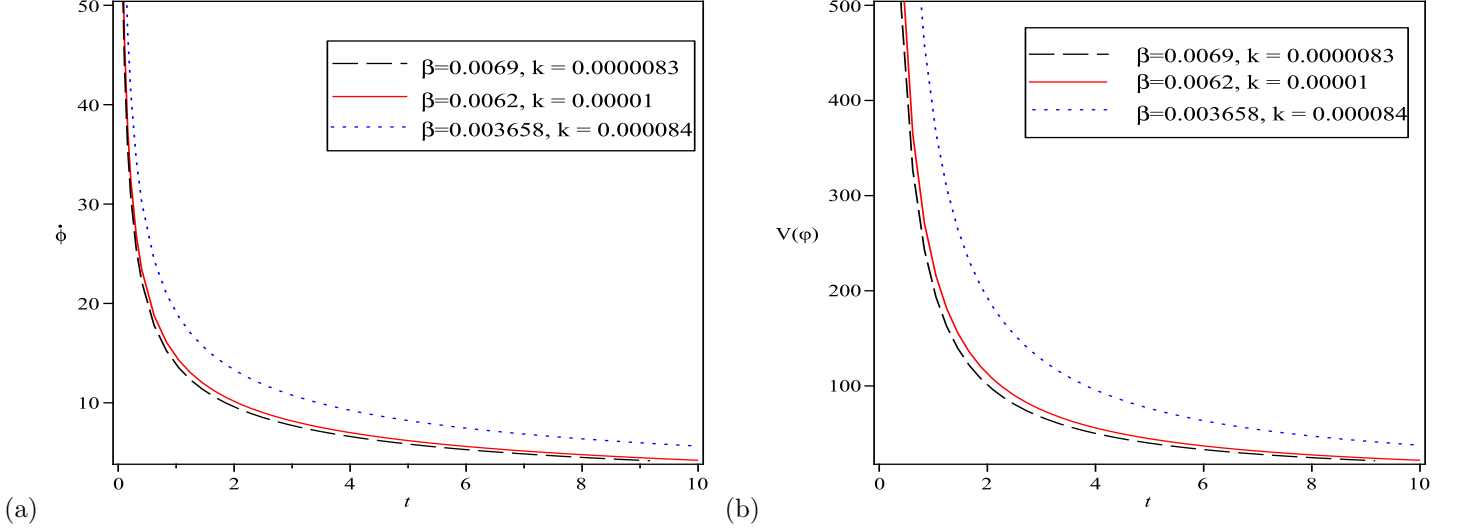


Figure 8: (a)The plot of left hand sides of scalar field versus time t , (b) The plot of potential versus cosmic time t .

A canonical scalar field ϕ describe the quintessence model. A slowly varying potential of scalar field $V(\phi)$ can lead to the accelerating Universe.

This method is close to slow inflation in the early Universe. But the difference is that it is not possible to ignore non-relativistic matter (dark matter and baryons) to accurately explain the nature of DE.

Figure (8a) shows the graph of scalar field ϕ with time t for all three values of β and k . Scalar field ϕ decreases through the evolution of time and tends to small positive value at the present epoch. Figure (8b) depicts potential of scalar field that correspond to LRS Bianchi type-I GGPDE model, which is also decreasing function of time

9 Concluding remarks

A new LRS Bianchi type-I generalized ghost pilgrim DE anisotropic universe with time dependent DP q and time dependent EoS parameter ω has been explored by new idea.

Here we have considered two assumptions: (i) σ^2 (shear scalar) $\propto \theta$ (scalar expansion) and (ii) the DP q as a linear function of H (Hubble parameter).

There are following main features of the model:

- For different purposes, like in analysis of jerk parameter, correspondence with various scalar field models, thermodynamics laws, the evolution of our universe by extracting different cosmological parameters, the generalized ghost dark energy model play a very important role. In different modified theories, various cosmological aspects of this model have been also addressed. It should be mentioned here that ρ_m (energy density of matter) and ρ_Λ (the proper energy density), are positive in the deduced model.
- The anisotropic parameter A_m is a constant and is non-zero for $m \neq 1$. ie. our model is anisotropic and may attain isotropy if $m = 1$.

- The interacting scenario of generalized ghost dark energy with CDM has been studied and cosmological parameters like jerk parameter, total energy density and equation of state parameter (EoS) have been evaluated by us. For three different well-known values of k and β , equation of state parameter (EoS) of PDE parameter has been explored. ω_Λ is in the phantom region of our universe for all three observational values of k and β .
- The GGPDE gives the dynamics of Ω given by Eq. (30). In this derived model, Ω is obtained as time dependent which is a positive decreasing with time and approach to 1 at present epoch (Figure 4).
- It is observed that the best suitable value of jerk parameter is very close to 1 at present time (Figure 5). This shows that our GGPDE model is very close to the Λ CDM model.
- The model represents that H , σ^2 and θ diverge at $t = -\frac{k}{2\beta}$, but the volume becomes unity at $t = -\frac{k}{2\beta}$. Hence, the GGPDE model starts expanding with a big bang singularity at $t = -\frac{k}{2\beta}$. It may be observed that when t tends to ∞ , the volume becomes ∞ .
- The GGPDE model represents an expanding, shearing, non-rotating and transit (from decelerating to accelerating) Universe.
- The squared sound speed trajectories demonstrate positive behavior throughout the evolution and model stability are also discussed in (Fig.6).
- For our GGPDE model, we also developed the $\omega_D - \omega'_D$ plane in (Fig.7) correspond to both thawing regions and freezing regions.
- Nevertheless, our model's trajectories differ mostly in the freezing region, as indicated by observational data (the expansion of the universe is comparatively more accelerated in the freezing region).
- We also observed the quintessence correspondence with a scalar field ϕ and potential $V(\phi)$ in (Fig.8a, 8b). For many different potentialities, the dynamics of quintessence in the presence of non-relativistic matter have been studied in detail [83, 88–91]. This result is a good agreement with the current scenario of the universe.

Hence, our constructed model and their solutions are physically acceptable. Therefore, for the better understanding of the characteristics within the framework of consistency GGPDE models, the solution demonstrated in this paper may be helpful.

References

- [1] D Saez and V J Ballester, *Phys. Lett. A* **113**, 467 (1986)
- [2] M S Berman, *Il Nuovo Cimento B* **74**, 182 (1983)
- [3] A G Reiss *et al*, *Astrophys. J.* **116**, 1008 (1998)
- [4] S Perlmutter *et al*, *Astrophys. J.* **517**, 565 (1999)
- [5] D N Spergel *et al*, *Astrophys. J. Suppl.* **148**, 175 (2003)
- [6] M Tegmark *et al*, *Astrophys. J.* **606** 702 (2004)
- [7] V U M Rao, M V Santhi, T Vinutha and G Sreedevi Kumari, *Int. J. Theor. Phys.* **51**, 3303 (2012)
- [8] V U M Rao, K V S Sireesha and P Suneetha, *African Rev. Phys.* **7**, 0054 (2012)
- [9] V U M Rao, K V S Sireesha and D Neelima, *ISRN Astron. Astrophys.* **2013** Article ID 924834, 11 (2013)
- [10] C L Bennett *et al*, *Astrophys. J. Suppl. Ser.* **148**, 1 (2003)
- [11] V U M Rao, T Vinutha and K M Vijaya Santhi, *Astrophys. Space Sci.* **314**, 213 (2008)
- [12] V U M Rao, V Santhi and T VinuthaK, *Astrophys. Space Sci.* **314**, 27 (2008)
- [13] R L Naidu *et al*, *Int. J. Theor. Phys.* **51**, 1997 (2012)
- [14] R L Naidu *et al*, *Astrophys. Space Sci.* **338**, 333 (2012)

- [15] V U M Rao and D Neelima, *Astrophys. Space Sci.* **345**, 427 (2013)
- [16] V U M Rao, K V S Sireesha and B J M Rao, *Prespacetime J.* **5**, 772 (2014)
- [17] V U M Rao, D C Papa Rao and D R K Reddy, *Astrophys. Space Sci.* **357**, 77 (2015)
- [18] V U M Rao and V Jayasudha, *Astrophys. Space Sci.* **358**, 8 (2015)
- [19] O Akarsu and C B Kilinc, *Astrophys. Space Sci.* **326**, 315 (2010)
- [20] O Akarsu and C B Kilinc, *Gen. Relativ. Gravit.* **42**, 763 (2012)
- [21] R Zia, U K Sharma and D C Maurya, *New Astronomy* **72**, 83 (2019)
- [22] A K Yadav, *Astrophys. Space Sci.* **335**, 565 (2011)
- [23] A Pradhan, R Jaiswal, K Jotania and R K Khare, *Astrophys. Space Sci.* **337**, 401 (2012)
- [24] T Singh and R Chaubey, *Pramana-J. Phys.* **71**, 447 (2008)
- [25] B Saha and A K Yadav, *Astrophys. Space Sci.* **341**, 651 (2012)
- [26] K S Adhav *et al*, *Astrophys. Space Sci.* **332**, 497 (2011)
- [27] S Sarkar and C R Mahanta, *Int. J. Theor. Phys.* **52**, 1482 (2013)
- [28] S Sarkar, *Gen. Relativ. Gravit.* **45**, 53 (2013)
- [29] S Sarkar, *Astrophys. Space Sci.* **349**, 985 (2014)
- [30] S Sarkar, *Astrophys. Space Sci.* **351**, 361 (2014)
- [31] G Varshney, U K Sharma and A Pradhan, *New Astronomy* **70**, 36 (2019)
- [32] L Susskind, *Jour. Math. Phys.* **36** (1995) 6377
- [33] S D H Hsu, *Phy. Lett. B* **594**, 13 (2014)
- [34] M Li, *Phys. Lett. B* **603**, 15 (2004)
- [35] A Cohen *et al*, *Phys. Rev. Lett.* **82**, 4971 (1999)
- [36] M R Setare, J Zhang and X Zhang, *JCAP* **03**, 007 (2007)
- [37] M Malekjani, A K Mohammadi and N N Pooya, *Astrophys. Space Sci.* **332**, 515 (2011)
- [38] Y Aditya and D R K Reddy, *Astrophys. Space Sci.* **363**, 207 (2018)
- [39] V U M Rao, G Suryanarayana and U D Prasanthi, *Bulletin Math. Statis. Res.* **5**, 48 (2017)
- [40] H Wei, *Class. Quantum Grav.* **29**, 175008 (2012)
- [41] E Babichev *et al*, *Phys. Rev. Lett.* **93**, 021102 (2004)
- [42] M Sharif and A Jawad, *Astrophys. Space Sci.* **351**, 321 (2014)
- [43] C R Mahantaa and N Sarmab, *New Astronomy* **57**, 70 (2017)
- [44] D D Pawar and S P Shahareab, *New Astronomy* **75**, 101318 (2020)
- [45] M S Singh and S Singh, *New Astronomy* **72**, 36 (2019)
- [46] A Jawad, *Eur. Phys. J. C* **74**, 3215 (2014)
- [47] A Jawad, V Debnath and F Batool, *Commun. Theor. Phys.* **64**, 590 (2015)
- [48] M V Santhi *et al*, *Astrophys. Space Sci.* **361**, 142 (2016)
- [49] M V Santhi *et al*, *Int. J. Theor. Phys.* **56**, 362 (2017)

- [50] V U M Rao and U Y D Prasanthi, *Can. J. Phys.* **95**, 554 (2017)
- [51] A Jawad, S Rani, I G Salako and F Gulshan, *Int. J. Mod. Phys. D* **26**, 1750049 (2017)
- [52] M Sharif and K Nazir, *Mod. Phys. Lett. A* **31**, 1650148 (2016)
- [53] E Ebrahimi, A Sheykhi and H Alavirad, *Cent. Europ. Jour. Phys.* **11**, 949 (2013)
- [54] C B Collins and J Wainwright, *Phys. Rev. D* **27**, 1209 (1983)
- [55] K S Thorne, *Astrophys. J.* **148**, 51 (1967)
- [56] P Garg, R Zia and A Pradhan, *Int. J. Geom. Methods Mod. Phys.* **16**, 1950007 (2019)
- [57] R K Tiwari, R Singh and B K Shukla, *African Rev. Phys.* **10**, 0048 (2015)
- [58] U K Sharma, R Zia, A Pradhan and A Beesham, *Res. Astron. Astrophys.* **19**, 4 (2018)
- [59] R K Tiwari, A Beesham and B K Shukla, *Int. J. Geom. Methods Mod. Phys.* **15**, 1850189 (2018)
- [60] J V Cunha, *Phys. Rev. D* **79**, 047301 (2009)
- [61] R Giostri *et al*, *J. Cosmol. Astropart. Phys.* **03**, 027 (2012)
- [62] H Amirshaschi and S Amirhashchi, arXiv:1802.04251 [astro-ph.co] (2018)
- [63] S Capozziello, O Farooq, O Luongo and B Ratra, *Phys. Rev. D* **90**, 044016 (2014)
- [64] S Capozziello, O Luongo and E N Saridakis, *Phys. Rev. D* **91**, 124037 (2015)
- [65] P Astier *et al*, *Astron. Astrophys.* **447**, 31 (2006)
- [66] T M Davis *et al*, *Astrophysical J.* **666**, 716 (2007)
- [67] A A Mamon, *Mod. Phys. Lett. A* **33**, 1850056 (2018)
- [68] R Nair *et al*, *JCAP* **01**, 018 (2012)
- [69] A A Mamon and S Das, *Int. J. Mod. Phys. D.* **25**, 1650032 (2016)
- [70] O Farooq and B Ratra, *Astrophys. J* **766**, L7 (2013)
- [71] J Magana *et al*, *JCAP* **10**, 017 (2014)
- [72] A A Mamon, K Bamba and S Das, *Eur. Phys. J. C* **77**, 29 (2017)
- [73] J A S Lima, J F Jesus, R C Santos and M S S Gill, arXiv: 1205.4688v3[astro-ph.CO] (2012)
- [74] A G Riess *et al*, *Astrophys. J.* **560**, 49 (2001)
- [75] L Amendola, *Not. R. Mon. Astron. Soc.* **342**, 221 (2003)
- [76] E Komatsu *et al*, *Astrophys. Jour. Suppl. Ser.* **180**, 330 (2009)
- [77] V Sahni, T D Saini, A A Starobinsky and U Alam, *Jour. Exper. Theor. Phys. Lett.* **77**, 201 (2003)
- [78] R D Rapetti, S W Allen, M A Amin and R D Blandford, *Mon. Not. Roy. Astron. Soc.* **375**, 1510 (2007)
- [79] A Mukherjee and N Banerjee, *Phys. Rev. D* **93**, 043002 (2016)
- [80] Z X Zhai, M J Zhang, Z-S Zhang, X-M Liu, and T-J Zhang, *Phys. Lett. B* **727**, 8 (2013)
- [81] J Q Xia, *Phys. Rev. D* **73**, 063521 (2006)
- [82] G B Zhao *et al*, *Phys. Rev. D* **72**, 123515 (2005)
- [83] R R Caldwell, E V Linder, *Phys. Rev. Lett.* **95**, 141301 (2005)
- [84] T Chiba, *Phys. Rev. D* **73**, 063501 (2006)

- [85] Z K Guo *et al.* *Phys. Rev. D* **74**, 127304 (2006)
- [86] M Malekjani, A K Mohammadi, *Int. J. Theor. Phys.* **51**, 3141 (2012)
- [87] V Sahnia, A Shafielooa and A A Starobinsky, arXiv:0807.3548v3 [astro-ph] (2008)
- [88] S Tsujikawa, *Class. Quant. Grav.* **30**, 214003 (2013)
- [89] E J Copeland, A R Liddle and D Wands, *Phys. Rev. D* **57**, 4686 (1998)
- [90] D L Macorra and G Piccinelli, *Phys. Rev. D* **61**, 123503 (2000)
- [91] E V Linder, *Phys. Rev. D* **73**, 063010 (2006)